Effect of lanthanide contraction on crystal structures of lanthanide coordination polymers with 2,5-piperazinedione-1,4-diacetic acid†

Gui-Lin Zhuang, Xiang-Jian Kong,* La-Sheng Long,* Rong-Bin Huang and Lan-Sun Zheng

Received 25th January 2010, Accepted 16th April 2010
DOI: 10.1039/c001537g

A series of lanthanide coordination polymers have been synthesized through the hydrothermal reaction of 2,5-piperazinedione-1,4-diacetic acid (H_2PODC) and $Ln(NO_3)_3$ (Ln = La, 1; Pr, 2; Sm, 3; Ho, 4 and Er, 5). Crystal structure analysis reveals that their structural variations are attributed to the effect of lanthanide contraction.

Lanthanide coordination polymers are of contemporary interest because of their fascinating structural diversity and unique properties.[1–7] Up to now, a great many lanthanide coordination polymers with interesting architectures and topologies have been obtained by selecting the appropriate ligands and controlling the reaction conditions.[1–7] However, the design of lanthanide coordination polymers with desired structures still remains a great challenge, not only because the assembly of the framework is frequently influenced by external physical or chemical stimuli, but also because of the high coordination number as well as the flexible coordination geometry of lanthanide ions.[1–7] In addition, less attention was paid to the influences of lanthanide contraction on the topological structure of lanthanide coordination polymers.[8,9]

Recently, we have found that the multifunctional ligand of 2,5-piperazinedione-1,4-diacetic acid (H_2PODC) can be obtained from the iminodiacetic acid with high yield under hydrothermal *in situ* reaction.[10] Based on the H_2PODC ligand (Scheme 1), we report the synthesis and characterization of five 3D structure lanthanide coordination polymers, $[Ln(PODC)_{1.5}(H_2O)]\cdot nH_2O$ (Ln = La (**1**), $n = 2$; Ln = Pr (**2**), $n = 1$; Ln = Sm (**3**), $n = 4$; Ln = Ho (**4**) and Er (**5**), $n = 2$). Although possessing same formula of $[Ln(PODC)_{1.5}(H_2O)]$, complexes **1–5** exhibit four distinct structural types. Their structural diversity reveals that lanthanide contraction plays an important role in the assembly of lanthanide coordination polymers.

Crystal analysis reveals that the asymmetric units of complexes **1–5** consists of one Ln(III) ion, one and half $PODC^{2-}$ ligands and one terminal aqua ligand.‡ It is noted that only the $PODC^{2-}$ ligand containing N3 atom in each unit cell of **2** and **3** lies on a crystallographic inversion centre, while all the $PODC^{2-}$ ligands in **1**, **4** and **5** lie on crystallographic inversion centres. Complex **1** crystallizes in space group $P\bar{1}$ of triclinic system. As shown in Fig.1a, the central La(III) ion locates in the center of a monocapped square antiprism geometry and is coordinated by one oxygen atom from terminal aqua molecule, one carbonylic oxygen atom from one $PODC^{2-}$ ligand, and seven carboxylic oxygen atoms from other six different $PODC^{2-}$ ligands, in which five carboxylic groups in unidentate fashion and one carboxylic group in chelating bidentate fashion. So, each La(III) ion bridges seven $PODC^{2-}$ ligands. The bond lengths of La–O range from 2.479 to 2.825(2) Å, comparable to those in the reported nonacoordinated La-complex.[11] Adjacent La(III) ions are linked by two carboxylic groups in $\mu_2:\eta^1:\eta^1$ and one carboxylic group in $\mu_2:\eta^2:\eta^1$ mode, generating a 1D {La-(COO)$_3$} chain along *a* axis (Fig.1b). Connection of adjacent chains through the $PODC^{2-}$ ligands produces 2D layer structure (Fig.1b). Adjacent 2D layers are linked *via* the carbonyl and carboxylic groups from different $PODC^{2-}$ ligands, alternately, extending into the 3D framework (Fig. 1c). The $PODC^{2-}$ ligands display two types of coordination modes (Scheme 1a and 1b), bridging five and four lanthanide ions, respectively.

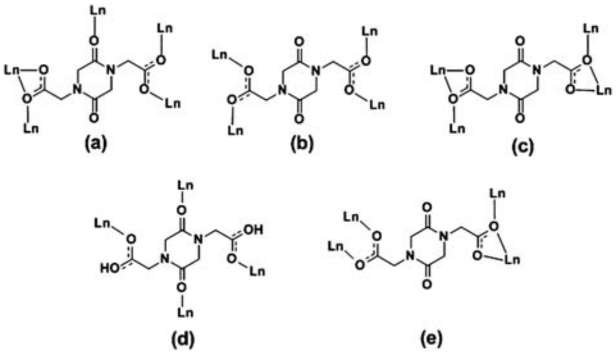

Scheme 1 The coordination mode of $PODC^{2-}$ ligand in **1–5**.

As shown in Fig. 2a, each Pr central in complex **2** is coordinated by one aqua ligand and six $PODC^{2-}$ ligands, in which two $PODC^{2-}$ ligands provide two carboxylate groups in chelating mode, three $PODC^{2-}$ ligands afford three carboxylate oxygen atoms in unidentate mode and one $PODC^{2-}$ ligand supply one carbonyl group. The bond length of Pr–O is range from 2.3896(19) to 2.631(2) Å, comparable to those value of the nonacoordinated Pr-complex.[12] Adjacent Pr(III) ions are linked by two carboxylic groups in $\mu_2:\eta^2:\eta^1$ mode, generating a 1D $\{Pr\text{-}(COO)_2\}_n$ along *a* axis (Fig. 2b), which is different from that in **1**. The 2D structure of **2** is similar to those of **1**, except that both of the two carboxylic groups adopt $\mu_2:\eta^2:\eta^1$ mode to link the adjacent Pr(III) ions. The 3D supramolecular architectures can be viewed as the 2D layer linked by two opposite carbonyl groups of $PODC^{2-}$, as shown in Fig. 2c. The $PODC^{2-}$ ligands in **2** act as μ_5- and μ_4-bridges (Scheme 1c and 1d), connecting five and four lanthanide ions, respectively.

The coordination environment of Sm(III) ion in **3** is shown in Fig. 3a. There are also six $PODC^{2-}$ ligands coordinated to one Sm(III) ion. Each Sm(III) ion is nonacoordinated, featuring coordination by four oxygen atoms from two carboxylate groups in

---

State Key Laboratory of Physical Chemistry of Solid Surface and Department of Chemistry, College of Chemistry and Chemical Engineering, Xiamen University, Xiamen, 361005, China. E-mail: lslong@xmu.edu.cn; Fax: +86 592 218 3047

† Electronic supplementary information (ESI) available: Details of synthesis for complexes **1–5**. CCDC reference numbers 763312–763315, 773687. For ESI and crystallographic data in CIF or other electronic format see DOI: 10.1039/c001537g

Table 1 Crystal data and details of data collection and refinement for complexes **1–4**

Complex	**1**	**2**	**3**	**4**	**5**
Formula	$C_{12}H_{18}O_{12}N_3La$	$C_{12}H_{16}O_{11}N_3Pr$	$C_{12}H_{22}O_{14}N_3Sm$	$C_{12}H_{18}O_{12}N_3Ho$	$C_{12}H_{18}O_{12}N_3Er$
M_r	535.20	519.19	582.68	561.22	563.55
Crystal system	Triclinic	Triclinic	Monoclinic	Triclinic	Triclinic
Space group	$P\bar{1}$	$P\bar{1}$	$P2_1/n$	$P\bar{1}$	$P\bar{1}$
a/Å	4.5588(2)	8.5017(3)	7.80280(10)	7.8133(3)	7.8393(16)
b/Å	11.9018(5)	9.4822(3)	19.2619(3)	10.7254(4)	10.837(2)
c/Å	15.8005(6)	10.8767(5)	12.6700(2)	11.9085(4)	11.905(2)
α/°	85.912(4)	106.740(4)	90	64.815(4)	64.88(3)
β/°	84.811(3)	101.306(4)	98.9750(10)	70.883(3)	71.67(3)
γ/°	83.249(3)	92.424(3)	90	72.769(3)	73.68(3)
V/Å^3	846.27(6)	818.80(5)	1880.94(5)	838.79(5)	856.4(3)
Z	2	2	4	2	2
D_c/g cm^{-3}	2.100	2.106	2.058	2.222	2.185
μ/mm^{-1}	2.599	3.045	3.204	4.792	4.974
Data/parameters	3276/253	3200/244	3675/271	3281/248	3234/253
θ/°	3.89–25.99	2.26–26.00	3.26–26.00	2.30–25.99	3.01–26.00
Observed reflections	2822	2858	3088	3120	3348
$R_1[I > 2\sigma(I)]^a$	0.0220	0.0194	0.0232	0.0147	0.0361
wR_2 (all data)^b	0.0505	0.0485	0.0836	0.0369	0.0983

^{a} $R_1 = \sum||F_o| - |F_c||/\sum|F_o|$. ^{b} w$R_2 = \{\sum[w(F_o^2 - F_c^2)^2]/\sum[w(F_o^2)^2]\}^{1/2}$.

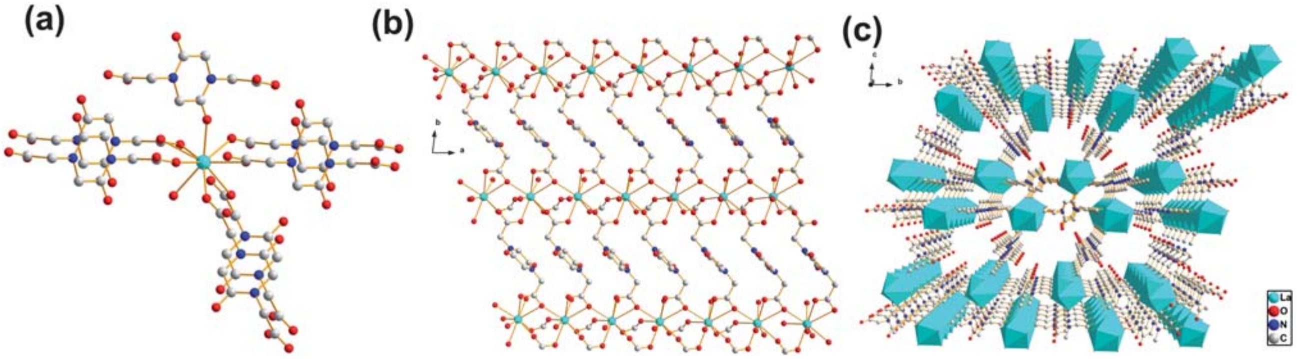

Fig. 1 (a) Coordination environment of the La^{3+} ion in **1**; (b) ball and stick view of the 2D structure of **1** along the *ab* face; (c) ball and stick plot showing the 3D structure of **1** (guest water molecules and hydrogen atoms are omitted for clarity).

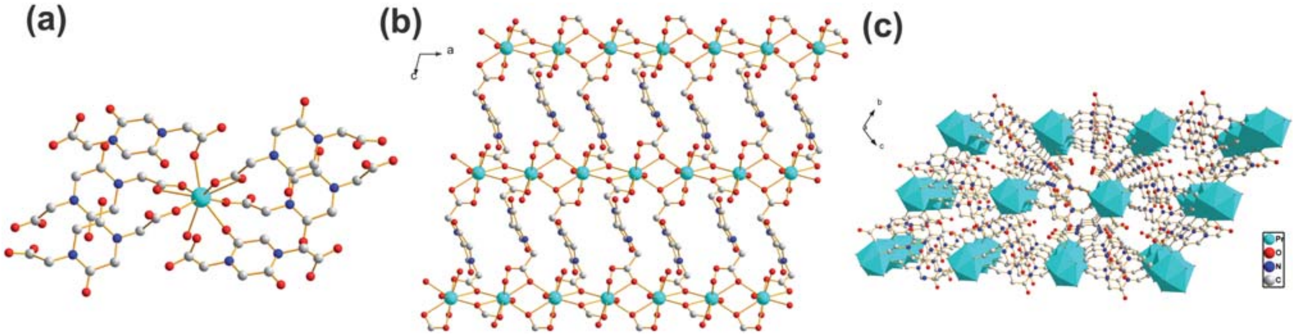

Fig. 2 (a) Ball and stick view of coordination environment of Pr^{3+} ion in **2**; (b) ball and stick view of the 2D structure of **2** along the *bc* face; (c) ball and stick view of the 3D structure of **2** (guest water molecules and hydrogen atoms are omitted for clarity).

chelating mode, four oxygen atoms from four carboxylate groups in unidentate mode and one aqua ligand. The bond length for Sm(III)–O is range from 2.349(4) to 2.635(3) Å, comparable to those of the nona-coordinated Sm-complex.[13] It is noted that the carbonyl group of PODC^{2-} ligand does not bond with the Sm(III) ions, which is different to those of **1** and **2**. Adjacent Sm(III) ions are linked by two carboxylate groups in μ_2:η^2:η^1 fashions and two carboxylate groups in μ_2:η^1:η^1 fashions, forming a dinuclear unit. Connection of the adjacent dinuclear units by two carboxylate groups in μ_2:η^2:η^1 fashions generate 1D $\{Sm\text{-}(COO)_4\text{-}Sm\text{-}(COO)_2\}_n$ chain along

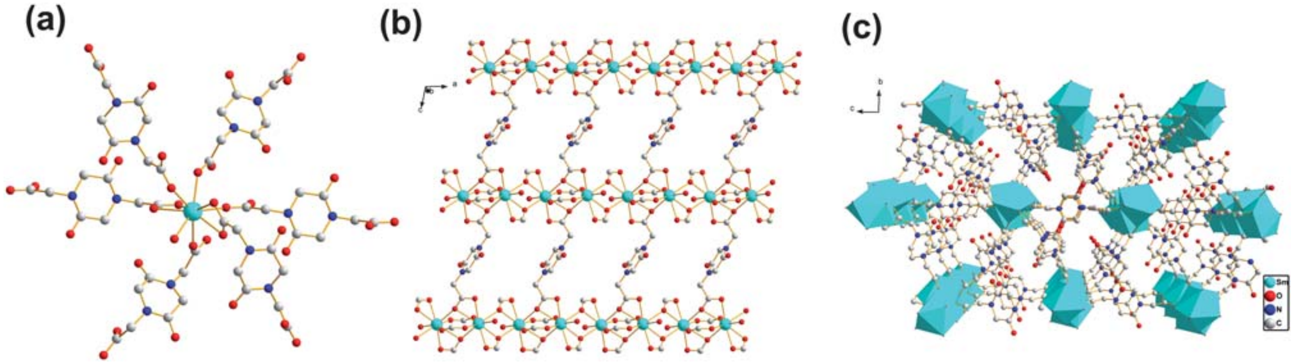

Fig. 3 (a) Coordination environment of Sm^{3+} in **3**; (b) ball and stick view of the 2D structure in **3** along the *ac* face; (c) ball and stick plot showing the 3D structure of **3** (guest water molecules and hydrogen atoms are omitted for clarity).

a axis(Fig. 3b). The 3D framework can be viewed as the 2D structure, which formed by connecting of adjacent chain along *b* axes *via* the two opposite carboxylate groups of $PODC^{2-}$, are linked by the $PODC^{2-}$ ligand (Fig. 3c). The $PODC^{2-}$ ligand shows two distinct coordination modes as shown in Scheme 1c and 1e.

As shown in Fig. 4a, the coordination environment of Ho(III) ion in **4** is similar to those of the Sm(III) in **3**, except for only one carboxylate groups in chelating mode coordinated to Ho(III) ion. The bond length for Ho–O range from 2.2410(18) to 2.5366(18) Å, comparable to those of the octa-coordinated Ho(III)-complex.[14] Adjacent Ho(III) ions are alternately linked by four carboxylate groups in μ_2:η^1:η^1 fashions and two carboxylate groups in μ_2:η^2:η^1 fashions, forming a 1D $\{Ho\text{-}(COO)_4\text{-}Ho(COO)_2\}_n$ chain. As shown in Fig. 4b and Fig. 4c, the 2D structure and 3D framework of **4** are constructed by the $\{Ho\text{-}(COO)_4\text{-}Ho(COO)_2\}$ chains, similar to those of **3**. The $PODC^{2-}$ ligand exhibits two different coordination modes as shown in Scheme 1b and 1c. Complex **5** is isostructural to **4**. The bond length for Er–O range from 2.240(4) to 2.540(4) Å, comparable to those of reported for Er-complex.[10]

Thermogravimetric analysis (TGA) studies were performed in a N_2 atmosphere at a heating rate of 10 °C min^{-1} for complexes **1–5**. As shown in the ESI, Fig. S2,† the TGA diagram of **1** displays an initial the weight loss of 9.8% between room temperature and 300 °C, which correspond to the removal of two guest water molecules and one aqua ligand (calcd 10.1%). Between 300 and 400 °C, **1** shows no weight loss, which is an indication of its stability up to 400 °C. When the temperature is higher than 400 °C, **1** rapidly decomposes. Similarly, the TGA curve of **2–5** display the first weight loss of 7.7% (calcd 7.0% for **2**), 12.2% (calcd. 12.3% for **3**), 9.6% (calcd. 9.7% for **4**) and 9.7% (calcd 9.6% for **5**), respectively, for the loss of the guest water molecules and aqua ligands. All the frameworks of **2–5** are stable up to 300 °C.

It is interesting to observe that the five complexes exhibit five different structures due to the different lanthanide ions, revealing that the effect of lanthanide contraction play an important role in the formation of complexes **1–5**. Based on the structure analysis, we found that lanthanide contraction has following influence on the structures of **1–5**. First, as the radii of the Ln ions decreases, the ligand–ligand repulsion increases. As the result of the repulsion, the numbers of ligands around the Ln ions decreases from seven (for **1**) to six (for **2–5**), and the coordination number also decreases from nine (for **1–3**) to eight (for **4** and **5**). Second, the average bond length of Ln–O decreases with decreasing the radii of the Ln ions. The average distances of Ln–O for **1–5** are 2.590, 2.526, 2.461, 2.364 and 2.358 Å, respectively. Third, the Lewis acidity of the Ln(III) ions increases as decreasing the radii of Ln(III) ions. Based on the theory of HSAB (Hard and Soft Acids and Bases),[15] carboxylate group tend to bond with the Ln(III) ions with harder Lewis acidity. Thus, The La(III) ions in **1** and Pr(III) ions in **2** coordinate to the carbonyl and carboxylate group, while Sm(III) ions in **3**, Ho(III) ions in **4** and Er(III) ions in **5** only coordinate to carboxylate group. In addition, the flexibility $PODC^{2-}$ ligands also affects the structures of the complexes. As shown in Scheme 1, the $PODC^{2-}$ ligand exhibits five distinct coordination modes. Their variable coordination modes also

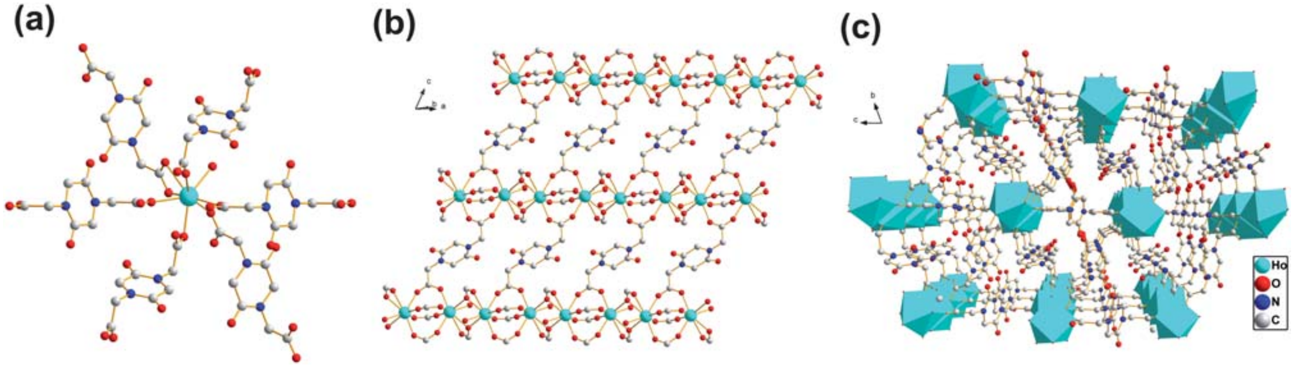

Fig. 4 (a) Coordination environment of Ho^{3+} in **4**; (b) ball and stick plot showing the 2D structure in **4** viewed along the ac face; (c) ball and stick plot showing the 3D structure of **4** (guest water molecules and hydrogen atoms are omitted for clarity).

induce the different topology frameworks, leading to the diversity of the structures of **1–5**.

In summary, we have reported a series of lanthanide coordination polymers based on 2,5-piperazinedione-1,4-diacetic acid under hydrothermal conditions. These coordination polymers crystallize in four different structural types with different lanthanide ions. Moreover, we also discussed the role of lanthanide contraction in the assembly of lanthanide-based coordination polymers.

Acknowledgements

We thank the NNSFC (grant no. 20825103, 20721001 and 20901064), the 973 project (grant 2007CB815304) from MSTC and the Natural Science Foundation of Fujian Province of China (grant no. 2008J0010) for the financial support.

Notes and references

‡ Single-crystal X-ray structure determination: Data collections were performed on an Oxford Gemini S Ultra CCD area detector using MoKα radiation at 173 K for complexes **1–4**. Absorption corrections were applied by using the multiscan program CrysAlis Red. Data of **5** was collected on a Rigaku RAXIS-APID detector at 173 K using MoKα radiation. The structures were solved by direct methods, and non-hydrogen atoms were refined anisotropically by least-squares on F^2 using the SHELXTL-97 program.[16] The hydrogen atoms of the organic ligand were generated geometrically (C–H, 0.96 Å). Crystal data as well as details of data collection and refinement for the complexes are summarized in Table 1.

1 O. Guillou and C. Daiguebonne, *Handbook on the Physics and Chemistry of Rare Earths*, vol. 34, Elsevier, Amsterdam, 2005.

2 (*a*) C. L. Cahill, D. T. de Lill and M. Frish, *CrystEngComm*, 2007, **9**, 15; (*b*) J. C. G. Bünzli, *Acc. Chem. Res.*, 2006, **39**, 53; (*c*) J. C. G. Bünzli and C. Piguet, *Chem. Rev.*, 2002, **102**, 1897; (*d*) H. C. Aspinall, *Chem. Rev.*, 2002, **102**, 1807.

3 (*a*) C. Marchal, Y. Filinchuk, X. Y. Chen, D. Imbert and M. Mazzanti, *Chem.–Eur. J.*, 2009, **15**, 5273; (*b*) T. Devic, C. Serre, N. Audebrand, J. Marrot and G. Férey, *J. Am. Chem. Soc.*, 2005, **127**, 12788; (*c*) X. J. Kong, Y. L. Wu, L. S. Long, L. S. Zheng and Z. P. Zheng, *J. Am. Chem. Soc.*, 2009, **131**, 6918.

4 (*a*) R. G. Xiong, J. Zhang, Z. F. Chen, X. Z. You, C. M. Che and H. K. Fun, *J. Chem. Soc., Dalton Trans.*, 2001, 780; (*b*) X. D. Gao, G. S. Zhu, Z. Y. Li, F. X. Sun, Z. H. Yang and S. L. Qiu, *Chem. Commun.*, 2006, 3172; (*c*) D. T. de Lill and C. L. Cahill, *Chem. Commun.*, 2006, 4946; (*d*) J. Zhao, L. S. Long, R. B. Huang and L. S. Zheng, *Dalton Trans.*, 2008, 4714; (*e*) D. F. Weng, X. J. Zheng, L. C. Li, W. W. Yang and L. P. Jin, *Dalton Trans.*, 2007, 4822.

5 (*a*) T. Gunnlaugsson and J. P. Leonard, *Chem. Commun.*, 2005, 3114; (*b*) X. J. Kong, L. S. Long, Z. P. Zheng, R. B. Huang and L. S. Zheng, *Acc. Chem. Res.*, 2010, **43**, 201; (*c*) C. M. G. dos Santos, A. J. Harte, S. J. Quinn and T. Gunnlaugsson, *Coord. Chem. Rev.*, 2008, **252**, 2512; (*d*) M. D. Allendorf, C. A. Bauer, R. K. Bhakta and R. J. T. Houk, *Chem. Soc. Rev.*, 2009, **38**, 1330.

6 (*a*) C. Benelli and D. Gatteschi, *Chem. Rev.*, 2002, **102**, 2369; (*b*) A. Mishra, W. Wernsdorfer, K. A. Abboud and G. Christou, *J. Am. Chem. Soc.*, 2004, **126**, 15648; (*c*) S. Osa, T. Kido, N. Matsumoto, N. Re, A. Pochaba and J. Mrozinski, *J. Am. Chem. Soc.*, 2004, **126**, 420; (*d*) C. M. Zaleski, E. C. Depperman, J. W. Kampf, M. L. Kirk and V. L. Pecoraro, *Angew. Chem., Int. Ed.*, 2004, **43**, 3912; (*e*) S. Tanase and J. Reedijk, *Coord. Chem. Rev.*, 2006, **250**, 2501.

7 (*a*) L. C. Silva, S. Lima, D. Anaias, P. Silva, L. Mafra, L. D. Carlos, M. Pillinger, A. A. Valente, F. A. A. Paz and J. Rocha, *J. Mater. Chem.*, 2009, **19**, 2618; (*b*) J. Y. Lee, O. K. Farha, J. Roberts, K. A. Scheidt, S. T. Nguyen and J. T. Hupp, *Chem. Soc. Rev.*, 2009, **38**, 1450.

8 (*a*) Q. D. Liu, S. Gao, J. R. Li, B. Q. Ma, Q. Z. Zhou and K. B. Yu, *Polyhedron*, 2002, **21**, 1097; (*b*) J. W. Cheng, S. T. Zheng and G. Y. Yang, *Dalton Trans.*, 2007, 4059; (*c*) S. N. Wang, R. Sun, X. S. Wang, Y. Z. Li, P. Yi, J. F. Bai, M. Scheer and X. Z. You, *CrystEngComm*, 2007, **9**, 1051; (*d*) J. Xia, B. Zhao, H. S. Wang, W. Shi, Y. Ma, H. B. Song, P. Cheng, D. Z. Liao and S. P. Yan, *Inorg. Chem.*, 2007, **46**, 3450; (*e*) X. J. Kong, Y. P. Ren, L. S. Long, R. B. Huang, L. S. Zheng and M. Kurmoo, *CrystEngComm*, 2008, **10**, 1309.

9 (*a*) M. Seitz, A. G. Oliver and K. N. Raymond, *J. Am. Chem. Soc.*, 2007, **129**, 11153; (*b*) L. Pan, X. Y. Huang, J. Li, Y. G. Wu and N. W. Zheng, *Angew. Chem., Int. Ed.*, 2000, **39**, 527; (*c*) A. Dimos, D. Tsaousis, A. Michaelides, S. Skoulika, S. Golhen, L. Ouahab, C. Didierjean and A. Aubry, *Chem. Mater.*, 2002, **14**, 2616; (*d*) Z. He, E. Gao, Z. Wang, C. Yan and M. Kurmoo, *Inorg. Chem.*, 2005, **44**, 862; (*e*) X. F. Li, Z. B. Han, X. N. Cheng and X. M. Chen, *Inorg. Chem. Commun.*, 2006, **9**, 1091; (*f*) H. L. Sun, C. H. Ye, X. Y. Wang, J. R. Li, S. Gao and K. B. Yu, *J. Mol. Struct.*, 2004, **702**, 77.

10 X. J. Kong, G. L. Zhuang, Y. P. Ren, L. S. Long, R. B. Huang and L. S. Zheng, *Dalton Trans.*, 2009, 1707.

11 H. Zhang, Z. L. Shen, T. Okamura, H. F. Zhu, W. Y. Sun and N. Ueyama, *Cryst. Growth Des.*, 2005, **5**, 1191.

12 C. Meyer and Z. Bromant, *Z. Anorg. Allg. Chem.*, 2003, **629**, 6.

13 Z. H. Zhang, T. Okamura, Y. Hasegawa, H. Kawaguch, L. Y. Kong, W. Y. Sun and N. Ueyama, *Inorg. Chem.*, 2005, **44**, 6219.

14 A. Lossin and G. Meyer, *Z. Anorg. Allg. Chem.*, 1993, **619**, 1609.

15 R. G. Pearson, *J. Am. Chem. Soc.*, 1963, **85**, 3533.

16 *SHELXTL 6.10*, Bruker Analytical Instrumentation, Madison, WI, 2000.